Study of a Series of Nb_3X Compounds by Nuclear Magnetic Resonance*

E. Ehrenfreund, A. C. Gossard, and J. H. Wernick
Bell Telephone Laboratories, Murray Hill, New Jersey 07974
(Received 23 June 1971)

A series of Nb_3X (X = Sn, Al, Au, Pt, Ir) compounds has been studied by observation of nuclear magnetic resonances between 4.2 and 300 °K. The full quadrupole structure of Nb^{93} NMR was observed by means of pulsed resonance techniques, while X-site resonances were also studied with steady-state techniques. Spin components of the magnetic susceptibility and Knight shift were deduced and found to be smaller and less temperature dependent than in the case of the V_3X compounds of comparable superconducting transition temperatures. The orbital term of the susceptibility (and the Knight shift) is found to be larger in compounds having higher density of states at the Fermi energy. An attempt is made to account for this correlation in terms of the Labbé-Friedel one-dimensional theory of the d-band structure. The linear relationship between the electric field gradient and the density of states at the Fermi energy found earlier in the V_3X series is not fulfilled in the Nb_3X series. An unusual increase in $1/(T_1T)$ slightly above the superconducting transition temperature is observed for Al^{27} nuclei in Nb_3Al. The possibility that superconducting thermal fluctuations are the source of this effect is considered.

I. INTRODUCTION

We have performed NMR measurements on several Nb_3X (X = Al, Sn, Au, Pt, Ir) compounds having the β-W lattice structure. The interest in these materials arises from their unusually high superconducting transition temperatures, their unusual band structure, and their singular elastic behavior. The vanadium-based A_3B compounds have been investigated thoroughly by NMR methods,[1-4] while the niobium-based ones have undergone only a few measurements.[5-7] The lack of NMR studies of the niobium-based compounds is mainly due to the large quadrupolar broadening of the resonance of the niobium nuclei in their noncubic A site. In the vanadium-based compounds, it was found that those compounds with high T_c show an unusual temperature dependence of the Knight shift K and the nuclear spin-lattice relaxation time T_1. The nonsuperconductors of that series showed no such anomalies. It is believed that a very narrow d band with high density of states at the Fermi energy is the cause for the above temperature dependences.[2] The narrow-d-band picture is supported by the postulated "one-dimensional" structure of the A sublattice in these A_3B compounds[8,9] and also by detailed band-structure calculations which show that because of the special structure, sections of the equal-energy surfaces are planar.[10,11] The situation with the niobium-based compounds is different; the Nb^{93} Knight shift in Nb_3Al (T_c = 18.7 °K) and Pt^{195} shift in Nb_3Pt (T_c = 8.5 °K) and magnetic susceptibilities in both these compounds are roughly temperature independent. The Sn^{119} Knight shift in Nb_3Sn (T_c = 18 °K) was found to be strongly temperature dependent; however, its behavior as a function of the temperature below ~ 50 °K is different from the recently measured magnetic susceptibility of Nb_3Sn.

II. EXPERIMENTAL TECHNIQUE

The samples of Nb_3Ir, Nb_3Au, Nb_3Sn, and Nb_3Pt were made by inert-electrode arc-melting together proper amounts of their components. The Nb_3Al samples were made by reacting compacted powder bars as described earlier by Willens *et al.*[6] X-ray powder diffraction patterns were taken to verify the crystal structure. The powders for the NMR measurements were obtained by crushing the ingots until the particle size was less than about 37 μ.

Since the Nb^{93} resonance is extremely quadrupolar broadened, the measurements were performed using the spin-echo technique in magnetic fields as high as 60 kOe. Spectra were obtained by recording the integrated spin-echo amplitude as a function of the external magnetic field at a constant frequency and fixed-pulse parameters. Magnetic fields were created using a superconducting solenoid. A magnetoresistance probe, made from thin copper wire and calibrated against the NMR of aluminum metal, was utilized to measure the field during an experiment. The reproducibility of this field determination is better than 0.03%. Steady-state techniques, using a Varian wide-line spectrometer operating at frequencies up to 16 MHz, were utilized in order to measure the narrow resonances of the X nuclei in the Nb_3X (X = Al, Sn) compounds. Spin-lattice relaxation times were measured from the recovery of the echo amplitude or free-induction decay following a saturating comb of rf pulses.

Measurement at temperatures 4.2, 14–20, 63, and 77 °K were done with boiling liquids. Temperatures other than the above between 20 and 150 °K were obtained by placing the sample in a heated

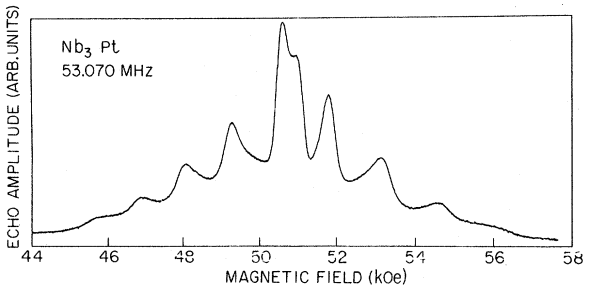

FIG. 1. Spin-echo spectrum of Nb^{93} in Nb_3Pt at constant frequency of 53.050 MHz and at 4.2 °K. The satellite structure seen is a typical quadrupole powder pattern of nuclei with spin $I=\frac{9}{2}$.

partially thermally isolated sample holder. For the wide-line spectrometer we used for the sample holder a quartz vial, machined from a single crystal of quartz and immersed in Al_2O_3 powder (as described elsewhere).[12] For the pulsed spectrometer we used instead an isolation Dewar with Al_2O_3 powder placed inside the liquid bath.

III. EXPERIMENTAL RESULTS

A. Line Shapes

The nuclear resonance spectra observed in our Nb_3X samples show the structure characteristic of nuclear electric quadrupole interactions[13] (Fig. 1). The observed patterns are typical of those expected in a powdered sample with an axially symmetric electric field gradient (efg) in high magnetic fields for nuclei of spin $I=\frac{9}{2}$. The expression for the frequency of the transition between the nuclear Zeeman states m_I and m_I-1, including anisotropic shift and correct for the second order, is[13,14]

$$\nu_{m_I}=\nu_0+\tfrac{1}{2}(m_I-\tfrac{1}{2})\nu_Q(3\cos^2\theta-1)+(1/32\nu_0)\nu_Q^2 f_m(\theta)\,,$$

where

$$\nu_0=\nu_R[1+K_{\rm iso}+K_{\rm ax}(3\cos^2\theta-1)]\,,$$

$$\nu_Q=3e^2qQ/2hI(2I-1)\,,$$

$$f_m(\theta)=\sin^2\theta\{[102m(m-1)-18I(I+1)+39]\cos^2\theta - [6m(m-1)-2I(I+1)+3]\}\,.$$

ν_R is the pure Zeeman frequency, ν_0 the transition frequency in the absence of the quadrupole interaction but including the anisotropic shift, ν_Q is a measure for the quadrupole interaction strength, and θ is the angle between the applied magnetic field H and the principal axis of the efg tensor. In powders all angles θ occur and the resonance line is broadened. In first order, neglecting for the moment the effect of anisotropic shift, intensity maxima occur for $\theta=\frac{1}{2}\pi$ giving rise to four satellite peaks (for the special case of $I=\frac{9}{2}$) on either side of the $\frac{1}{2}\leftrightarrow-\frac{1}{2}$ central transition. In second order, the central transition is also split, with intensity maxima occurring at $\theta=\frac{1}{2}\pi$ and $\theta=\cos^{-1}(5/9)^{1/2}$, and the satellite peaks are shifted equally in pairs. Including now the anisotropic shift $K=K_{\rm iso}+K_{\rm ax}\times(3\cos^2\theta-1)$, its main effect is on the second-order term, since its angular dependence $(3\cos^2\theta-1)$ is the same as that of the first-order term. It changes the splitting between the central transition peaks in such a way that for positive $K_{\rm ax}$ the spacing between the peaks is reduced, while for negative $K_{\rm ax}$ it is increased. The actual expression for the spacing between the peaks is

$$\Delta\nu_{1/2}=\frac{25}{6}\frac{I(I+1)-\frac{3}{4}}{24}\frac{\nu_Q^2}{\nu_R}-\frac{5}{3}K_{\rm ax}\nu_R+\frac{1}{6}\frac{K_{\rm ax}^2\nu_R^3}{\nu_Q^2}\,.$$

The field difference between symmetrically spaced satellite peaks on opposite sides of the central transition then gives the values of ν_Q, and the center of gravity of each pair when corrected for the second-order shift of this pair gives the Knight shift for nuclei with magnetic fields perpendicular to the symmetry axis $[K(\theta=\frac{1}{2}\pi)\equiv K_\perp]$. The spacing $\Delta\nu_{1/2}$, together with the deduced ν_Q gives the anisotropy of the shift $K_{\rm ax}$. However, in our case of the Nb_3X compounds there are a certain number (of order of 1%) of the Nb nuclei situated on cubic sites. Only in the case of Nb_3Al is the second-order shift at 50 MHz large enough to distinguish between the two $\frac{1}{2}\leftrightarrow-\frac{1}{2}$ second-order splitting peaks and the cubic site peak. In the other compounds we could not distinguish conclusively between the cubic site peaks and the second-order peaks of the central transition. At frequencies lower than about 60 MHz the central linewidth is dominated by the second-order quadrupole splitting rather than by the shift anisotropy. Thus, working at frequencies below 60 MHz we could only determine the shift anisotropy of Nb^{93} in Nb_3Al: $K_{\rm ax}=+(0.15\pm0.10)\%$. By investigating the line shape of the other samples, we estimated $K_{\rm ax}$ to be positive in all cases and smaller than that in Nb_3Al. The Nb^{93} Knight shifts deduced according to the above analysis of the line shape are shown as a function of temperature in Fig. 2. The quadrupole coupling constants, which appeared to be temperature independent within the experimental error, are shown in Table I.

Observations of nuclear spin-echo signals in the mixed superconducting state of these type-II superconducting powdered samples was possible because of the penetration of the external dc and rf magnetic fields. However, determination of the Knight shifts suffers because of shielding effects due to supercurrents. These effects were not taken into account and thus the Knight shift results are subject to a relatively large negative error in the superconducting state.

The quadupolar satellite structure is a very sen-

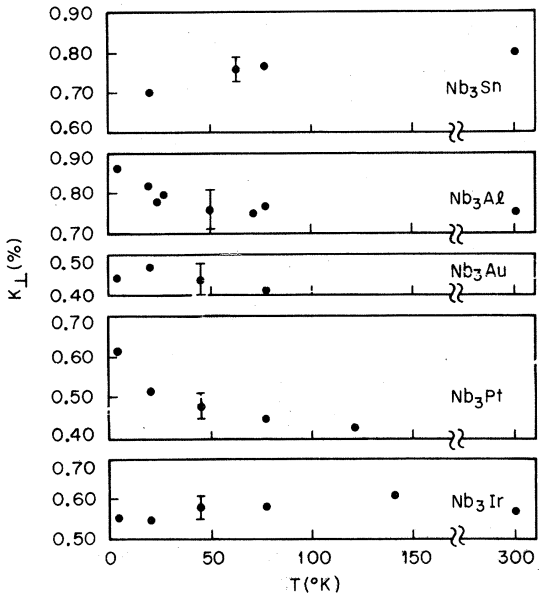

FIG. 2. Nb^{93} $K_\perp$ vs temperature for the Nb_3X compounds. The superconducting transition temperatures for the investigated samples are Nb_3Sn: 17.7 °K, Nb_3Al: 18.2 °K (annealed), 16 °K (quenched) (there is no significant difference in $K_\perp$ for the annealed and quenched samples), Nb_3Au: 11.4 °K, Nb_3Pt: 8.5 °K, Nb_3Ir: 1.85 °K.

sitive probe for structural transformation in metals. For example, in V_3Si [12] the difference in e^2qQ between the two sites created after the structural transformation is some 50 times larger than their difference in the c/a ratio because of the redistribution of the conduction electrons associated with the transformation. Nb_3Sn is known to be transformed from high-temperature cubic structure to low-temperature tetragonal structure at ~40 °K. [15] This transformation reflects itself by washing out the satellite structure between 63 and 20 °K (Fig. 3). Examination of the satellite structure of the line profiles of the other samples Nb_3Ir, Nb_3Pt, Nb_3Au, and Nb_3Al shows that there is no detectable change which may indicate a structural transformation between 4 and 300 °K.

We have also measured the Al^{27} and Sn^{119} resonances in Nb_3Al and Nb_3Sn, respectively. Since the Al and Sn sites are cubic, no quadrupole broadening is expected and the resonance lines appear to be symmetric. A steady-state technique with small modulation fields (~ 5 G) was utilized to observe these sharp lines and prevent superposition of the much wider Nb^{93} resonances. The Al^{27} linewidth (between derivative extrema) is 7.9 ± 0.2 G, and its Knight shift, as a function of temperature, is given in Fig. 4. It is seen that the temperature dependence of the shift is small: The difference $[K^{27}(300\,°\mathrm{K}) - K^{27}(20\,°\mathrm{K})]$ is, at most, 0.08%. The Sn^{119} Knight shift, on the other hand, is much more temperature dependent (Fig. 4). However, unlike the previous published results, [5] it is not a monotonically increasing function of temperature but rather has a minimum in the vicinity of 40 °K. The magnetic susceptibility of a sample of Nb_3Sn which transforms at ~ 45 °K from cubic to tetragonal shows[16] the same behavior; above ~ 50 °K it is a monotonic decreasing function of temperature, but in the vicinity of the transformation temperature it has a maximum and below it decreases as the temperature decreases. Since not every Nb_3Sn sample undergoes structural transformation, depending on the preparation manner, it is believed that the previous data[5] were taken on a nontransforming sample. The Sn^{119} linewidth also shows temperature dependence; above ~ 40 °K it is constant, but it increases below this temperature (Fig. 4). The signal-to-noise ratio of our signal does not permit us to calculate the second moment or make a detailed analysis of the line shape. Since in the tetragonal phase of Nb_3Sn, below ~ 40 °K, the point symmetry of the Sn atoms is less than cubic, anisotropy of the Knight shift of the Sn^{119} nuclei ($I=\frac{1}{2}$) can occur and broaden the low-temperature line. This anisotropic Knight shift broadening and inhomogeneity of the polarization due to incomplete transformation or varying degrees of transformation, are the probable reasons for the observed broadening.

B. Relaxation Rates

Since the Nb^{93} spectra in the Nb_3X compounds investigated here are enormously wide, it is very difficult to determine experimentally the spin-lattice relaxation times. Complete saturation was impossible to achieve with our rig and as a result of only partial saturation the recovery is composed of several exponential terms, as expected for quadrupolar broadened lines. [17–19] We estimated upper and lower limits to T_1 in the following way: The longest relaxation time in the recovery must be no longer than the intrinsic T_1, whereas the shortest one in the case of a magnetic hyperfine relaxation process cannot be less than $T_1/I(2I+1)$. The result for Nb^{93} in Nb_3Al and Nb_3Sn at 20 °K is $250 \geq T_1^{93} \gtrsim 80$ msec.

For determination of T_1 of Al^{27} in Nb_3Al we used the fact that the free-induction decay time (T_2^*) for the wide Nb^{93} resonance is very short (< 1 μsec) compared with that of the narrow Al^{27} resonance

TABLE I. Measured quadrupole coupling constants for Nb_3X compounds.

	Nb_3Ir	Nb_3Pt	Nb_3Au	Nb_3Al	Nb_3Sn
$\lvert h^{-1}e^2qQ\rvert$ (MHz)	70 ± 1	64 ± 1	60 ± 1	107 ± 3	49 ± 1

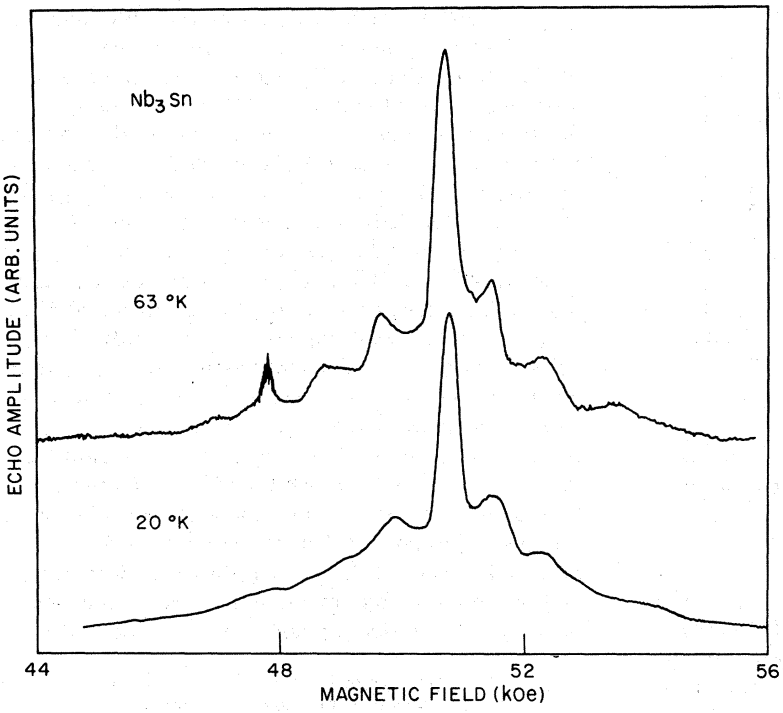

FIG. 3. Nb^{93} spin-echo spectra of Nb_3Sn at 63 °K (cubic phase) and 20 °K (tetragonal phase). At the tetragonal phase there are two nonequivalent Nb sites and the spectrum is the superposition of two spectra each with different efg and K. The wiggly peak at 47.88 kOe arises from aluminum metal put into the sample as a reference.

($\gtrsim 50$ μsec). The recovery of the free-induction decay tail after saturation by a number of narrow rf pulses was nearly exponential. In Fig. 5 we plot the behavior of $(T_1^{27}T)^{-1}$ as a function of temperature between 14 and 77 °K. Above 20 °K, T_1^{27} varies nearly as T_1^{-1} with $(T_1^{27}T)^{-1} = 0.065 \pm 0.005$ (sec °K)$^{-1}$. Below 20 °K $(T_1^{27}T)^{-1}$ possesses a peak in the vicinity of 17 °K. The data shown are for a quenched sample with smeared transition temperature; measured by an inductive method, 80% of the change in the inductance occurs between 14.2 and 16.0 °K while the rest of the change is smeared slightly above and below this range. At the operating field of ~ 50 kOe, T_c should drop by ~ 2 °K. An annealed sample of Nb_3Al with much sharper transition (0.5 °K wide) and higher T_c (18.2 °K) shows similar behavior with the peak at the vicinity of 18.5 °K. The highest known T_c for Nb_3Al is 18.7 °K at zero field.[6] Thus, it appears that the peak in $(T_1^{27}T)^{-1}$ occurs *above* $T_c(H)$, and thus, it presents an anomaly. A similar anomaly of $(T_1T)^{-1}$ has been observed previously in the related compounds V_3Si, V_3Ge, and V_3Pt.[4]

IV. DISCUSSION

A. Analysis of Susceptibility and Nb^{93} Knight Shift

Our measurements of Knight shifts and relaxation times allow us to determine the relative contributions to the magnetic susceptibility of the compounds. As is commonly done in the transition metals, we shall separate the susceptibility into

$$\chi = \chi_s + \chi_d + \chi_{orb} + \chi_{dia},$$

where χ_s, χ_d, χ_{orb}, and χ_{dia} are, respectively, the s-band electrons' spin susceptibility, d-band spin susceptibility, d-band orbital susceptibility, and the diamagnetic term due to the ion cores. An upper limit for χ_s and for the s density of states is derived from our T_1 measurement using Korringa's

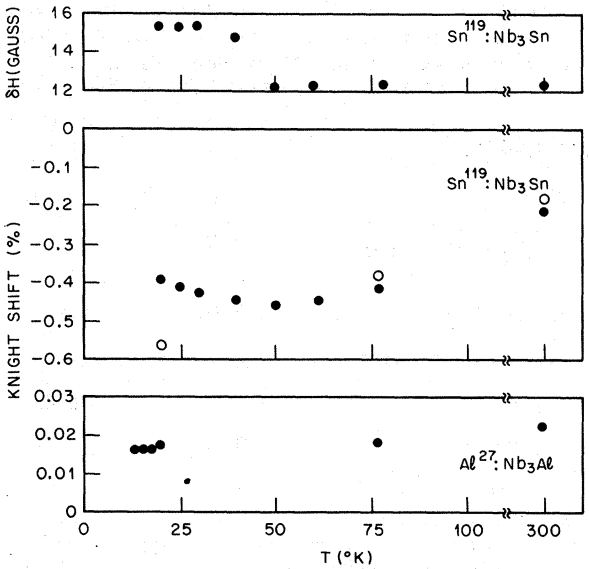

FIG. 4. Knight shifts and linewidth (δH) as a function of temperature of Al^{27} and Sn^{119} in Nb_3Al and Nb_3Sn, respectively. Open circles ○ (for Sn^{119} shift) were taken from Ref. 5, and probably represent the shift for nontransforming sample.

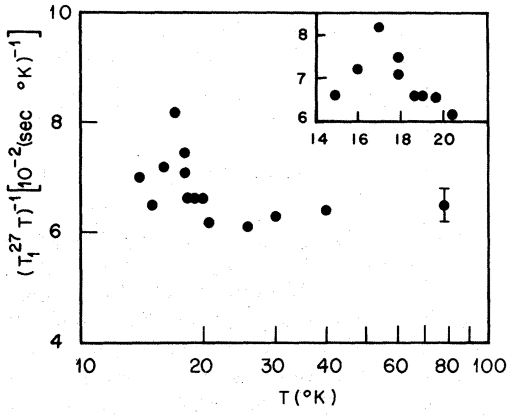

FIG. 5. $(T_1T)^{-1}$ vs T for Al^{27} in Nb_3Al in the range 14–77 °K and in a magnetic field of ~50 kOe. The anomalous behavior near T_c is illustrated in more detail in the right upper corner inset.

relation and the fact that $(T_1^{-1})_{\text{expt}} \geq (T_1^{-1})_{s\ \text{band}}$. Using $H_{hf}(5s) = 2.5\times10^6$ Oe/μ_B[20] for the 5s electron hyperfine field, we get for the s density of states $\eta_s(E_F) \leq 0.07$ (eV)$^{-1}$ per Nb atom, and for the susceptibility $\chi_s \leq 12\times10^{-6}$ emu per mole (i.e., per Avogadro's number of Nb_3X units). χ_d is derived from specific-heat density of states using corrections for the derived s density of states and corrections for electron-phonon and electron-electron interactions.[21] We shall assume $\chi_{dia} = -30\times10^{-6}$ emu/mole. Thus, we can estimate χ_{orb} from the above equation for the susceptibility, provided that the total susceptibility is known. We tabulated the values of χ_d and χ_{orb} derived in this way in Table II. The values of K_d^{93} and K_{orb}^{93} can be derived from the associated susceptibilities by using an estimate of values for the hyperfine fields. Assuming the same hyperfine field for Nb in all these compounds, we take $H_{hf}(4d\ \text{spin}) = -0.2\times10^6$ Oe/μ_B[20,22] (derived from EPR data of Nb^{4+}, Mo^{4+}, and Tc^{3+} in ionic crystals) and $H_{hf}(4d\ \text{orb}) = 0.29\times10^6$ Oe/μ_B.[20] Assuming $K_s = 0.10\%$ (the upper limit for K_s, using our T_1 measurements, is 0.14%) we may add $K_s + K_d + K_{orb}$ to get the total expected Knight shift. These values and the measured values of the Knight shift appear in the last two rows of Table II. (The *absolute* accuracy of the measured shift is ~0.1%.) In comparing the last two rows, it can be said that the analysis is not too arbitrary, and the main terms, d spin and d orbital, are reasonable. It is interesting to note that in every compound the orbital component of the susceptibility is dominant, and that compounds having higher transition temperatures have also higher orbital susceptibilities.

B. Discussion of Results in Terms of Labbe-Friedel One-Dimensional Band Model

The Labbê-Friedel (LF) one-dimensional band model[9] for the A_3B compounds having the β-W structure has been successful in explaining unusual features of some of the compounds which have the higher transition temperatures. Here we want to concentrate on the magnetic properties dictated by the model and to discuss the d-orbital and d-spin

TABLE II. Estimated susceptibilities and Knight shifts for various Nb_3X compounds. Included also, specific-heat coefficients γ and density of d states derived using these γ and McMillan electron-phonon coupling constant λ. All susceptibilities are given in 10^{-6} emu per mole (i.e., per Avogadro's number of Nb_3X units).

	Nb_3Os	Nb_3Ir	Nb_3Pt	Nb_3Au	Nb_3Al	Nb_3Sn
γ [mJ/mole (deg K)^2]	9.6[a]	8.8[a]	22[a]	37[a]	30[b]	62[c]
λ[d]	0.43	0.48	0.78	0.88	1.15	1.15
$\eta_d(E_F)\left(\frac{\text{states}}{\text{eV (Nb atom)}}\right)$	0.44	0.38	0.85	1.35	0.97	2.0
χ_d	80	70	154	246	177	370
$\chi_{meas}(0\ °K)$	420[e,f]	344[e,f]	500[e,f]	660[e,f]	635[b]	1000[g]
$\chi_{orb} \equiv \chi_{meas} - (\chi_d + \chi_{dia} + \chi_s)$	358	292	364	432	476	648
K_d (%)	−0.10	−0.09	−0.20	−0.32	−0.23	−0.49
K_{orb} (%)	0.62	0.51	0.63	0.75	0.86	1.14
$K_{tot} = K_s + K_d + K_{orb}$ (%)	0.62	0.52	0.53	0.53	0.73	0.75
$K_{meas}(0\ °K)$ (%)		0.55	0.54	0.47	0.82	0.70

[a]P. Spitzli, R. Flükiger, F. Heiniger, and J. Muller, Phys. Letters 30A, 170 (1969).

[b]Reference 6.

[c]F. J. Morin and J. P. Maita, Phys. Rev. 129, 1115 (1963).

[d]W. L. McMillan, Phys. Rev. 167, 331 (1968).

[e]Reference 7.

[f]D. I. Bardos, R. M. Waterstrat, T. J. Rowland, and J. B. Darby, J. Low Temp. Phys. 3, 509 (1970).

[g]Reference 16. The value for $T = 0$ °K was determined by extrapolation of the *cubic* phase susceptibility.

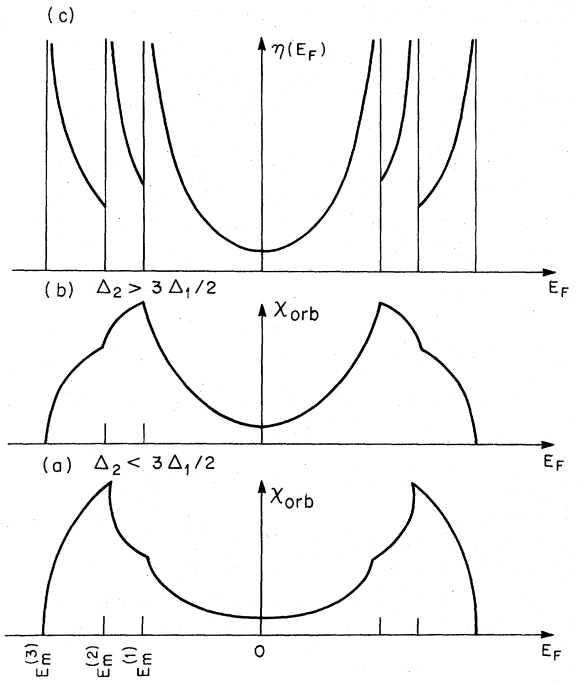

FIG. 6. Illustration of the variations of the orbital susceptibility and density of d states at E_F with the position of E_F in the d band (Ref. 23). It appears that in the range $E_m^{(1)} < E_F \leq 0$, χ_{orb} is a monotonic nondecreasing function of E_F.

susceptibilities.

The orbital part of the susceptibility has been calculated for the LF model and discussed as a function of the position of the Fermi level in the d band.[23] Typical results are illustrated in Fig. 6 together with the calculated density of d states at the Fermi energy as a function of its position in the d band. It is seen that there is a correlation between χ_{orb} and $\eta_d(E_F)$; in the range $E_m^{(1)} < E_F < 0$, χ_{orb} should be an increasing function of $\eta_d(E_F)$. In Fig. 7 we have plotted the experimentally analyzed χ_{orb} versus the density of states. One can see that χ_{orb} has a tendency to increase with increasing density of states. Thus, although the positioning of E_F above $E_m^{(1)}$ for these compounds has not yet been definitely proven, the present results tend to support such a model.

The temperature dependence of the susceptibility may arise from χ_{orb} and χ_d. In the LF model χ_{orb} is strongly changing with the position of E_F because of the special structure of the d band. For different positions of E_F the interval Δ between the levels responsible for χ_{orb} ranges between zero and $|E_m^{(1)} - E_m^{(2)}|$, and thus *a priori* one may expect the temperature dependence of χ_{orb} to be relatively large for certain values of Δ, and different for different positions of E_F.[23] As we shall show in the Appendix, the temperature dependence of χ_{orb} in the LF model is very small when $E_F \approx 0$ and much larger when E_F is close to the band edge in the range 0–300 °K. However, the change in χ_{orb}, expressed by $[\chi_{orb}(10\,^\circ\mathrm{K}) - \chi_{orb}(300\,^\circ\mathrm{K})]/\chi_{orb}(10\,^\circ\mathrm{K})$ does not exceed 5% in any case.

The d-spin part of the susceptibility is proportional to the density of states at the Fermi energy. Thus, in the LF model more temperature dependence is expected for materials with higher d-spin susceptibility, since for them the Fermi energy lies closer to the band edge. When E_F is close to the band edge, the d-spin susceptibility decreases with increasing temperature for the normal state in the cubic phase ("negative temperature dependence"); when E_F is far away from the band edge, the temperature dependence is much smaller, but the d-spin susceptibility should increase with increasing temperature ("positive temperature dependence") in this model.[23] For Nb_3Sn, in the cubic phase above 45 °K, there is a negative temperature dependence of the susceptibility[16] with $\chi(50\,^\circ\mathrm{K}) - \chi(300\,^\circ\mathrm{K}) \approx 140\times10^{-6}$ emu/mole and the Nb^{93} and Sn^{119} Knight shifts become less negative at higher temperatures. In Nb_3Sn, E_F lies very close to the band edge.[9] Thus, the large and negative temperature dependence of the susceptibility is accounted for by the LF model. The less negative K values at higher temperatures are explained by the negative core-polarization hyperfine field which induces these shifts. For Nb_3Au, the temperature dependence of χ is much smaller $[\chi(10\,^\circ\mathrm{K})\,\chi(300\,^\circ\mathrm{K}) \approx 80\times10^{-6}$ emu/mole$]$[7] and that of the K is less than our experimental error bar (Fig. 2). We believe that this temperature dependence is caused by the d-spin susceptibility, which is less temperature dependent than that of Nb_3Sn since $\eta(E_F)$ is smaller and E_F is not so close to the band edge. For Nb_3Pt the situation is different: χ is slightly negatively temperature dependent $[\chi(100\,^\circ\mathrm{K}) - \chi(300\,^\circ\mathrm{K}) \approx 20\times10^{-6}$ emu/mole$]$ and K^{93} is definite-

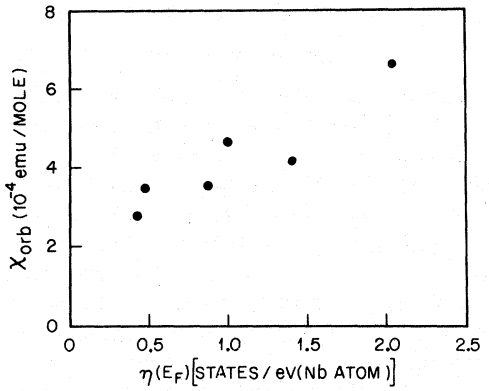

FIG. 7. Experimental χ_{orb} vs $\eta_d(E_F)$ with the various Nb_3X compounds as an implicit parameter (see Table II).

ly temperature dependent and becomes *less* positive at higher temperatures. Such a behavior of K^{93} may arise by positive temperature dependence of χ_d (and negative hyperfine field), possibly in combination with the negative temperature dependence of χ_{orb} (and positive hyperfine field). Since $\eta(E_F)$ for Nb_3Pt is much smaller than those for Nb_3Sn and Nb_3Au, E_F should lie far above the band edge in the LF band scheme. Thus, we suggest a slight positive temperature dependence of χ_d and a slight negative temperature dependence of χ_{orb} in order to explain the behavior in Nb_3Pt. For example, $\chi_d(300\,^\circ\mathrm{K}) - \chi_d(10\,^\circ\mathrm{K}) \approx 40\times10^{-6}$ emu/mole and $\chi_{orb}(10\,^\circ\mathrm{K}) - \chi_{orb}(300\,^\circ\mathrm{K}) \approx 20\times10^{-6}$ emu/mole can approximately account for the susceptibility and Knight shift behavior in Nb_3Pt. For Nb_3Al the situation seems to be similar to that of Nb_3Pt. A slight negative temperature dependence of χ_{orb} may also explain the smallness of the K^{93} change in Nb_3Sn and Nb_3Au.

When E_F is very close to E_m, structural transformation from a high-temperature cubic phase to a low-temperature tetragonal phase may occur.[9] The total spin susceptibility of the sample should decrease, since the narrow d band near E_F is split with one of the subbands created becoming empty at low temperatures. Such a behavior has been observed by Cohen *et al.*[16] in Nb_3Sn, which undergoes a structural transformation at $\sim 45\,^\circ\mathrm{K}$. The absolute value of our Sn^{119} Knight shift in Nb_3Sn (Fig. 4) also shows the same behavior. Since this shift should be linear with χ_d, it appears that the over-all temperature behavior of $|K^{119}|$ is due to a very narrow d band with the Jahn-Teller splitting at $\sim 40\,^\circ\mathrm{K}$.

Since for the calculation of χ_{orb} one needs the wave functions of all d bands, we could apply neither the Cohen-Cody-Halloran single d-band model[16] nor the Matheiss APW energy-band calculation[24] for the considerations in this section. The oversimplified one-dimensional LF band model seems to account for the features of the magnetic data in this series of compounds.

C. Hyperfine Interactions

It was shown above that the relaxation time measurement put an upper bound of 0.07 states per eV per Nb atom for one spin direction for the 5s electrons of the Nb. Now using a free-electron model for the s electrons of Nb in Nb_3Al and Nb_3Sn, assuming one s electron per Nb atom, we find $\eta_s(E_F)/\eta_{\mathrm{fr\ el}}(E_F) < 0.25$. Furthermore, $(T_1T)^{-1}$ of Al^{27} in Nb_3Al is only 0.065 $(\mathrm{sec}\,^\circ\mathrm{K})^{-1}$ in the normal state; this is 8 times smaller than $(T_1T)^{-1}$ for aluminum metal. Thus, it is apparent that the s density of states at the Fermi level is very small. This can be explained by the general picture of the APW band calculation for the A_3B compounds,[24] where the A and B s and p orbitals form narrow bands below and above the Fermi energy ("bonding" and "antibonding" bands), but their fractional character in bands near the Fermi energy is small.

For the Al^{27} in Nb_3Al we expect no orbital interaction and thus we interpret the Knight shift and relaxation as arising from s contact and core polarization only. We assume

$$K = K_s + K_{cp} \quad (K_{cp} < 0)\,,$$

$$T_1^{-1} = T_{1s}^{-1} + T_{1cp}^{-1}\,.$$

Using the Korringa-like relations for each term[20]

$$(T_1T)_i^{-1} = (4\pi k_B \gamma_n^2/\hbar\gamma_e^2) K_i q_i\,, \quad i = s,\ \mathrm{cp}$$

where q_i is the reduction factor for the process i ($q_s = 1$, $q_{cp} \leq 1$), we can calculate the different contributions by assuming a certain value for q_{cp}. In Table III we list the calculated values for $q_{cp} = 1$ and $q_{cp} = \frac{1}{3}$. It is apparent that the dominant relaxation process arises from the s-contact interaction.

D. Electric Field Gradients

The efg in metals is the sum of point charge, core and conduction electron contributions. In transition metals with relatively high density of states the conduction electron term plays an important role, and thus the measured efg may reflect some characteristics of the Fermi surface.

In V_3X compounds it was observed experimentally that the density of states at the Fermi level $\eta(E_F)$ scales with the efg, $|eq|$[25]; higher $|eq|$ values were found in compounds with higher $\eta(E_F)$. A large $\eta(E_F)$-dependent term of $|eq|$ was calculated in Ref. 25 and was proposed as the dominant term in the V_3X compounds. Now we have found that in Nb_3X compounds there is no such scaling (see Table I): Nb_3Sn, for example, which has the highest $\eta(E_F)$ in this series has the smallest $|eq|$ value. The absence of scaling between $|eq|$ and $\eta(E_F)$ on moving from one Nb_3X compound to another indicates that the predominant field-gradient term here is not simply proportional to the state density. Apparently, for Nb_3X, the assumptions of gradual state density changes and gradual wave function character changes with energy needed to obtain a linear dependence of $|eq|$ on $\eta(E_F)$ are

TABLE III. Conduction electron contributions to the relaxation rate and Knight shift for Al^{27} in Nb_3Al.

Interaction	$(T_1^{27}T)^{-1}$ $(\mathrm{sec}\,^\circ\mathrm{K})^{-1}$		$K^{27}(\%)$	
	$q_{cp}=1$	$q_{cp}=\frac{1}{3}$	$q_{cp}=1$	$q_{cp}=\frac{1}{3}$
Contact	0.051	0.059	+0.042	+0.045
Core polarization	0.014	0.006	−0.022	−0.025

not satisfied.

Using the most recent published values of the quadrupole moment for niobium[26] and vanadium,[27] we compare $|eq|$ values for the two series of compounds. It is seen from Table IV that $|eq|$ for the Nb-based A_3B compounds is some 10 times larger than those for the respective (with the same B atom) vanadium-based compounds. Possible sources for the difference in $|eq|$ values between Nb_3X and V_3X series appearing in Table IV are as follows: (i) The quadrupole moment values are subject to large errors (say, ~ 50%);[26,27] (ii) the lattice potentials might be different since they depend on the effective charge of the different sites and are a result of a severe cancellation. Also, the s electron screening might affect these quantities.

E. Nuclear-Spin Lattice Relaxation in Nb_3Al near T_c

In the normal state of a metal T_1T is usually a constant as a function of temperature.[28] Temperature dependence of T_1T in the normal state may result when the density of states is a strongly varying function of energy in a range $\sim k_BT$ near the Fermi energy. It may also arise as a result of a structural transformation that shifts the Fermi level in the band. It is likely that changes in T_1T because of these reasons would be accompanied by similar changes in related quantities such as Knight shift, susceptibility, and (for structural transformation) the electric field gradient.

In Nb_3Al a temperature dependence of $(T_1^{27}T)^{-1}$ is observed between 14 and 20 °K (Fig. 5). It is not accompanied, however, by a similar variation of the Knight shift (Fig. 4): K^{27} is constant within ~ 5% of its 20 °K value. Furthermore, investigating the quadrupolar structure of Nb^{93} NMR on our powdered sample at various temperatures we did not find any evidence for a structural transformation; also, Willens *et al.*[6] using x rays and optical techniques did not find any evidence for structural transformation in various samples of Nb_3Al. Thus, we believe that the variation of $(T_1^{27}T)^{-1}$ in Nb_3Al between 14 and 20 °K is not caused by effects of a very narrow band or structural transformation.

TABLE IV. Quadrupole coupling constant and efg's for several Nb_3X and V_3X compounds.

Compound	$\frac{e^2qQ}{h}\left(\frac{Mc}{s}\right)$	$\lvert eq\rvert$ (10^{14} cgs) [a]
Nb_3Ir	70	48
Nb_3Pt	64	44
Nb_3Au	60	41
Nb_3Sn	49	34
V_3Ir	1.0[b]	3.3
V_3Pt	1.0[b]	3.3
V_3Au	1.5[b]	5.0
V_3Sn	0.8[b]	2.7
Nb_3Al	107	74
V_3Si	2.9[b]	9.6
V_3Ga	3.2[b]	10.6

[a] For the nuclear quadrupole moments we used $Q^{93} = -0.2$ b (Ref. 26) and $Q^{51} = -0.04$ b (Ref. 27).

[b] Reference 25.

Since this variation of $(T_1T)^{-1}$ is occurring in the vicinity of T_c ($\Delta T/T_c \sim 10$–30%), one is encouraged to take into account effects of thermodynamic fluctuation of the order parameter. In a bulk (i.e., with dimensions much bigger than the coherence length ξ_0) dirty ($l < \xi_0$, l the electronic mean-free path) superconductor, Maki has calculated the enhancement in T_1^{-1} due to fluctuations above T_c in the so-called "classical regime" (at temperatures not too close to T_c, where the fluctuations are of classical type) and it is given by[29]

$$\frac{T_{1N}}{T_1} \approx 1 + a\left(\frac{T_c}{T - T_c}\right)^{1/2} , \tag{1}$$

where T_{1N} is the relaxation time in the normal state neglecting the effect of fluctuations. The coefficient a is given by

$$a = (k_B/32\pi\hbar^3)^{1/2} D^{-3/2} \eta^{-1}(E_F) T_c^{1/2} .$$

The transition temperature T_c is available by direct measurements; $\eta(E_F)$, the density of states per unit volume for single spin direction, is obtained from specific-heat measurements; $D = \frac{1}{3} l v_F$ is the diffusion constant and may be obtained from H_{c2}-vs-T measurements using the relation[30] $H_{c2}(T \approx T_c) = 4\varphi_0 k_B (T_c - T)/\pi^2 \hbar D$, where φ_0 is the flux quantum. Thus, for Nb_3Al using $T_c \approx 15$ °K $(dH_{c2}/dT)_{T \approx T_c} = -25 \times 10^3$ Oe/°K [31] and $\eta(E_F) = 1.0$ eV^{-1} (Nb atom)$^{-1}$ [6] $= 2.7 \times 10^{34}$ $erg^{-1}cm^{-3}$, we get $a = 1.8 \times 10^{-2}$. A value of $\approx 5 \times 10^{-2}$ for a in Eq. (1) is needed in order to explain the magnitude of the effect in Nb_3Al. This estimate for the fluctuation effect is applicable for isotropic superconductors. For Nb_3Al this model cannot be applied directly and a more realistic model is needed. In the limiting case when the linear-chain model can be applied to Nb_3Sn,[32] Nb_3Al, etc. the superconductor is very anisotropic. It has been suggested[33] that in the limiting one-dimensional case the characteristic length is of atomic size instead of the "mean free path" in the Maki formulation. Thus, the effect of fluctuation might be more favorable in superconductors of the β-W type of structure than in more isotropic bulk superconductors.

ACKNOWLEDGMENTS

We wish to acknowledge helpful discussions with and suggestions from V. Jaccarino, M. Weger, T. H. Geballe, and R. H. Willens. We thank R. H. Willens also for providing the Nb_3Al sample,

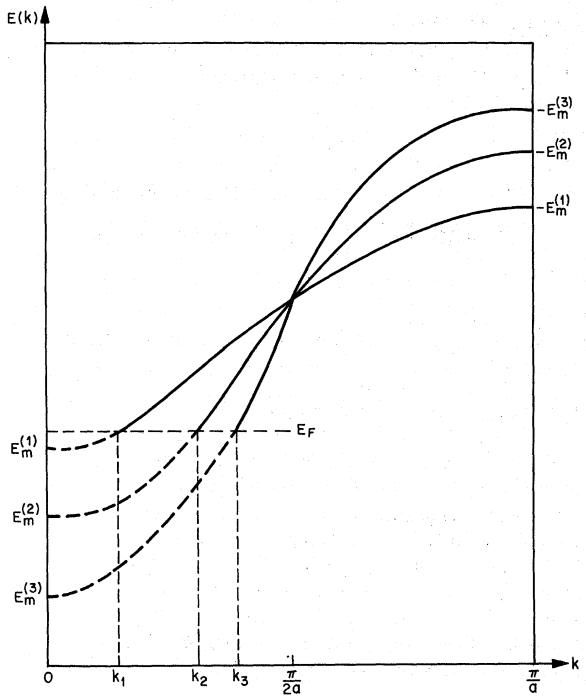

FIG. 8. E-vs-k diagram for the d bands in the LF linear chain model (Ref. 23).

G. W. Hull, Jr. for verifying the superconducting transition temperatures, and J. B. Mock for his valuable technical assistance.

APPENDIX: TEMPERATURE DEPENDENCE OF THE LF ORBITAL SUSCEPTIBILITY

The orbital susceptibility for the LF band structure is given by[23]

$$\chi_{orb} = \frac{4\mu_B^2 Na}{\pi}\left(4\int_0^{\pi/a}\frac{f[E_2(k)]-f[E_1(k)]}{E_1(k)-E_2(k)}\,dk + 6\int_0^{\pi/a}\frac{f[E_3(k)]-f[E_2(k)]}{E_2(k)-E_3(k)}\,dk\right), \quad \text{(A1)}$$

where $3N$ is the total number of Nb nuclei, $E_i(k) = E_m^{(i)}\cos ka$ are the d-band energies in the linear chain model (Fig. 8), $f(E) = \{1+\exp[\beta(E-E_F)]\}^{-1}$ is the Fermi distribution function with $\beta = (k_BT)^{-1}$, and a is the lattice constant. For finite temperatures χ_{orb} can be evaluated only numerically, by assuming certain numerical values for the parameters $E_m^{(i)}$ $(i=1, 2, 3)$ and $E_F(T=0)$ and taking into account the temperature dependence of E_F in the LF model[23] (the latter is important only when E_F is very close to $E_m^{(i)}$). We have computed χ_{orb} from Eq. (A1) in the range of temperatures 0–300 °K for various sets of parameters such that $1 < |E_m^{(1)}| < 5$ eV, $|E_m^{(1)} - E_m^{(2)}| > 0$, $|E_m^{(2)} - E_m^{(3)}| > 0$, and $0 \le |E_F(T=0)| < 0.93\,|E_m^{(1)}|$. We have found that for these sets of parameters χ_{orb} is a decreasing function of temperature in this range of temperatures and that its temperature dependence varies strongly with E_F. For $E_F \approx 0$ (i.e., near the middle of the band) the temperature dependence is 1–3 orders of magnitude less than when E_F is close to the band edge. In any case, the temperature dependence between 10 and 300 °K, expressed by $[\chi_{orb}(10)-\chi_{orb}(300)]/\chi_{orb}(10)$, did not exceed 5%.

*A preliminary account of this work is given in Solid State Commun. 8, 1925 (1970).
[1]W. E. Blumberg, J. Eisinger, V. Jaccarino, and B. T. Matthias, Phys. Rev. Letters 5, 149 (1960).
[2]A. M. Clogston and V. Jaccarino, Phys. Rev. 121, 1357 (1961).
[3]A. M. Clogston, A. C. Gossard, V. Jaccarino, and Y. Yafet, Phys. Rev. Letters 9, 262 (1962).
[4]B. G. Silbernagel, M. Weger, W. G. Clark, and J. H. Wernick, Phys. Rev. 153, 535 (1967).
[5]R. G. Shulman, B. J. Wyluda, and B. T. Matthias, Phys. Rev. Letters 1, 278 (1958).
[6]R. H. Willens, T. H. Geballe, A. C. Gossard, J. P. Maita, A. Menth, G. H. Hull, Jr., and R. R. Soden, Solid State Commun. 7, 837 (1969).
[7]M. Bernasson, P. Descouts, R. Flükiger, and A. Treyvaud, Solid State Commun. 8, 837 (1970).
[8]M. Weger, Rev. Mod. Phys. 36, 173 (1964).
[9]J. Labbé and J. Friedel, J. Phys. (Paris) 27, 153 (1966).
[10]M. Weger, J. Phys. Chem. Solids 31, 1621 (1970).
[11]I. B. Goldberg and M. Weger, Bull. Israel Phys. Soc. (to be published).
[12]A. C. Gossard, Phys. Rev. 149, 246 (1966).
[13]See, for example, M. H. Cohen and F. Reif, in *Solid State Physics*, edited by F. Seitz and D. Turnbull (Academic, New York, 1957), Vol. 5, p. 321.
[14]W. H. Jones, Jr., T. P. Graham, and R. G. Barnes, Phys. Rev. 132, 1898 (1963).
[15]R. Mailfert, B. W. Batterman, and J. J. Hanak, Phys. Letters 24A, 315 (1967).
[16]R. G. Cohen, G. C. Cody, and J. J. Halloran, Phys. Rev. Letters 19, 840 (1967).
[17]E. R. Andrew and D. P. Tunstall, Proc. Phys. Soc. (London) 78, 1 (1961).
[18]W. W. Simmons, W. J. O'Sullivan, and W. A. Robinson, Phys. Rev. 127, 1168 (1962).
[19]A. Narath, Phys. Rev. 162, 320 (1967).
[20]Y. Yafet and V. Jaccarino, Phys. Rev. 133, A1630 (1964).
[21]W. L. McMillan, Phys. Rev. 167, 331 (1968).
[22]W. Low, J. Appl. Phys. 39, 1246 (1968).
[23]J. Labbé, Phys. Rev. 158, 647 (1967).
[24]L. F. Mattheiss, Phys. Rev. 138, A112 (1965).
[25]R. E. Watson, A. C. Gossard, and Y. Yafet, Phys. Rev. 140, A375 (1965).
[26]K. Murakawa, Phys. Rev. 98, 1285 (1955).
[27]K. Murakawa, J. Phys. Soc. Japan 21, 1466 (1966).
[28]J. Korringa, Physica 16, 601 (1950).
[29]K. Maki, Progr. Theoret. Phys. (Kyoto) 40, 193

(1968).
[30]P. G. de Gennes, *Superconductivity* (Benjamin, New York, 1966), p. 270.
[31]S. Foner, E. J. McNiff, Jr., B. T. Matthias, T. H. Geballe, R. H. Willens, and E. Corenzwit, Phys. Letters 31A, 349 (1970).
[32]M. Weger, Solid State Commun. 9, 107 (1971).
[33]M. Weger (private communication).

PHYSICAL REVIEW B VOLUME 4, NUMBER 9 1 NOVEMBER 1971

Characteristic Temperatures of the Mössbauer Fraction and Thermal-Shift Measurements in Iron and Iron Salts*†

L. Dwynn Lafleur‡ and Clark Goodman
Department of Physics, University of Houston, Houston, Texas 77004
(Received 21 June 1971)

Mössbauer spectra have been measured in metallic iron, sodium nitroprusside, sodium ferrocyanide, and potassium ferrocyanide absorbers between 78 and 293 °K. The temperature dependences of the Mössbauer fraction f_a and the resonant velocity V_0 were fitted to Einstein and Debye lattice-vibration models. The characteristic temperatures of the models fitted to f_a are consistently lower than those fitted to V_0, showing the sensitivity of f_a to low-frequency modes of vibration. The characteristic temperatures obtained from V_0 are higher for the salts than for the metal, indicating the presence of higher-frequency modes in the salts. This interpretation is verified semiquantitatively by comparing the thermal-shift Debye temperatures of the salts to their infrared absorption frequencies. The Mössbauer fraction of potassium ferrocyanide shows a weaker temperature dependence than expected for a harmonic solid which suggests potassium ferrocyanide is anharmonic in the temperature range studied.

I. INTRODUCTION

The Mössbauer effect has been used by several investigators to study thermal-vibration properties of solids. Specifically, measurements of the Mössbauer (recoilless) fraction and the thermal shift in resonant γ energy are directly related, respectively, to the mean-square displacement and mean-square velocity of the Mössbauer nucleus in the solid. These studies fall into two general categories—source measurements and absorber measurements. In the former, the Mössbauer nucleus is usually present as a dilute impurity in the host lattice, so that information is obtained regarding the lattice-dynamical properties of an impurity atom in a solid. In the case of absorber studies, the Mössbauer nucleus is most often a major constituent of the solid, and measured properties are more directly dependent on the vibrational modes of the entire lattice.

Because the 14.4-keV γ-ray transition of Fe^{57} exhibits a strong Mössbauer effect in most materials even at room temperature, most of these studies have used that isotope. For example, Steyert and Taylor[1] studied sources consisting of the parent isotope Co^{57} diffused into several metal lattices. They were able to fit Mössbauer fraction measurements with Debye models for the lattice except at high temperatures ($\gtrsim$600 °K) where diffusion and anharmonicity were significant. Thermal-shift measurements were also fitted with Debye models and showed consistently lower Debye temperatures than those obtained from the Mössbauer-fraction measurements. Better agreement was obtained when Einstein models were used, indicating perhaps the presence of a localized mode of vibration of the source nucleus.

Very few Mössbauer-fraction measurements in absorbers have been fitted to lattice-dynamical models. Herber and Wertheim[2] have measured relative Mössbauer fractions in powdered ferrocine absorbers at temperatures from 20 to 295 °K. The results are interpreted as indicating contributions to the Mössbauer fraction from both optic and acoustic modes of vibration, but no fits to models are given. Kerler[3] measured Mössbauer fractions in metallic iron and several iron compounds at temperatures from 153 to 353 °K. Within the accuracy of his data, all temperature dependences were linear, indicating a temperature range near the classical Dulong-Petit limit. Debye temperatures were calculated for the iron metal and the salts.

Preston *et al.*[4] studied the Mössbauer spectrum of metallic iron absorbers from 4 to 1300 °K. Measurements of the thermal shift were fitted to a Debye model in the low-temperature region. At high temperatures, there was a definite deviation from the Dulong-Petit limit which they interpreted as a temperature-dependent isomer shift. (Their thermal-shift data have recently been reexamined by Housley and Hess.[5])

More recently, Johnson and Dash[6] measured Mössbauer fractions and thermal shifts in powdered